SOLUTION MINING RESEARCH INSTITUTE
105 Apple Valley Circle
Clarks Summit, PA 18411, USA

Telephone: +1 570-585-8092
Fax: +1 505-585-8091
www.solutionmining.org

Technical Conference Paper

Effects of Changes in the Cavern Pressure and Wellbore Temperature during a Liquid-Liquid MIT

Sivaprasath Manivannan, LMS, Ecole Polytechnique, Palaiseau, France

Pierre Bérest, LMS, Ecole Polytechnique, Palaiseau, France

Benoît Brouard, Brouard Consulting, Paris, France

SMRI Fall 2015 Technical Conference
28 – 29 September 2015
Santander, Spain

EFFECTS OF CHANGES IN THE PRESSURE AND TEMPERATURE OF THE TESTING FLUID DURING A LIQUID-LIQUID MIT

Manivannan S. and Bérest P., LMS, Ecole Polytechnique, France

Brouard B., Brouard Consulting, France

Abstract

Every year, hundreds of mechanical integrity tests (MITs) are performed worldwide. A large amount of literature has been dedicated to various technical aspects of MITs. The Solution Mining Research Institute (SMRI) suggested a reference for interpreting the results of an MIT (Crotogino, 1996). However, especially in densely inhabited areas of Europe, there is a growing public concern about the safety of underground storage; when performing tests, higher accuracies are currently required.

One objective of current research is to achieve a 1-cm resolution in the measurement of interface displacement. In such a context, a precise mathematical description of the test is required. Skaug et al. (2011) and Lampe and Ratigan (2014) have discussed the influence of transient disequilibrium in the vertical distribution of temperature in the wellbore. The present paper concerns the effects of cavern pressure and wellbore transient temperatures in the case of a Liquid-Liquid MIT and how they affect MIT results both when the standard method (logging tool) and the pressure-differential method are used.

1. POT, MIT, LLI and PD

Tightness is a pre-requisite for any hydrocarbon storage. A great asset of hydrocarbon storage in salt caverns, when compared to natural gas or CO_2 storage in depleted reservoirs or aquifer layers, is that tightness tests can be performed before commissioning and during the operating life of a cavern. Several kinds of tests were or currently are used: the Pressure Observation Test (POT), the (nitrogen) Mechanical Integrity Test (MIT), the Liquid-Liquid Interface test (LLI) and the Pressure Differential (PD) method.

The Pressure Observation Test (POT) is the simplest (and coarsest) testing method. The cavern is filled with liquid (brine, in most cases); cavern pressure is increased to the testing pressure through liquid injection; after injection, wellhead pressure evolution is monitored for several days. A rapid pressure-drop rate is deemed to be a clear sign of poor tightness. More precisely, if βV is the cavern compressibility, during a rapid injection, $\beta V = \Delta V / \Delta P$ is the ratio between the volume of liquid injected in the cavern (ΔV) and the resulting pressure increase (ΔP). Cavern compressibility equals the cavern volume (V) multiplied by the cavern compressibility factor (β), which is the sum of the

compressibility factor of brine plus the compressibility factor of the "hole", typically, $\beta = 4 \times 10^{-4}$ /MPa (or $\beta = 3 \times 10^{-6}$ /psi). When the pressure-drop rate (in MPa/day, for instance) is $\dot{P}$, the leak rate is deemed to be $\dot{v}_{leak} = -\beta V \times \dot{P}$. This test is too coarse, as many other factors (other than an *actual* leak) contribute to the observed pressure-drop rate, including pre-existing brine warming, additional dissolution, "reverse" creep, etc. (Van Sambeek et al., 2005). Cases were reported in which wellhead pressure *increased* during the test (Vrakas, 1988), suggesting that the leak was *negative!*

In the early 1980s (Lampe and Ratigan, 2014), a much more reliable testing method was developed and implemented by the cavern industry, the Mechanical Integrity Test (MIT), Figure 1, left. The cavern is filled with brine, but a testing fluid (nitrogen, in most cases) is injected in the annular space to develop a brine/testing-fluid interface below the last cemented casing shoe. Interface depth is tracked through a logging tool.

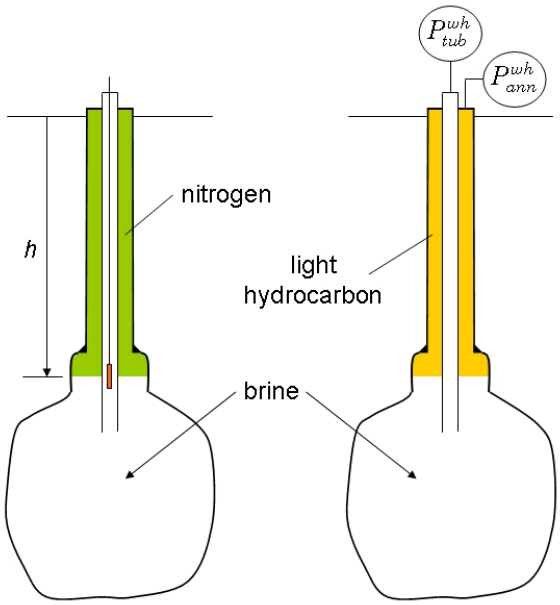

Figure 1. The Nitrogen MIT and the Liquid-Liquid Interface Test (LLI) using the Pressure Differential method. [In the former, the nitrogen/brine interface is tracked through a logging tool. In the latter, pressures of the brine-filled tubing and of the liquid-filled annular are recorded continuously at the wellhead during the test.]

The computed leak rate $(\dot{v}_{leak} > 0)$ is related to the interface rise rate $(\dot{h} < 0)$ by the simple relation $\dot{v}_{leak} = -\dot{h}\Sigma(h)$, where $\Sigma(h)$ is the annular cross-sectional area at interface depth. It sometimes is accepted that the duration of the MIT, Δt, and the accuracy of the interface displacement measurement, Δh, must be such that

$$\frac{\Sigma(h)\delta h}{\Delta t} < 1000 \text{ bbls/yr} \approx 450 \text{ liters/day}$$

The usual accuracy of standard logging tools is 15 cm (6 in), making $\delta h = 0.3$ m (Two measurements are needed.); $\Sigma(h) = 1\ \mathrm{m}^2$ is typical. In such a context, uncertainties with magnitudes of a few dozens of liters are not significant. The test is more sensitive when the annular cross-sectional area is smaller and the test duration longer.

However, in some cases, a higher resolution and more accurate tools are needed. Meinecke et al. (2013) describe a case in which the interface was monitored continuously with an ultrasonic logging tool, providing an accuracy rating of 25.8 liters/day; Langlinais and Moran (2008) used a downhole camera to monitor the nitrogen/brine interface during an MIT, resulting in a minimum detectable leak rate of 58 bbls/yr or 25 liters/day. In the spirit of the SMRI standardization effort achieved by Crotogino (1996), Geostock (personal communication) considers that the accuracy of MITs should be better than 50 kg/day (≈ 65 liters/day) for gasoil and 150 kg/day for nitrogen.

In addition to interface logging, the Pressure Differential (PD) method, first suggested by Diamond et al. (1993), can be used. This method (Figure 1 right) is based on wellhead pressure measurements (Bérest et al., 2001); and is explained in the next Section.

Nitrogen is the preferred testing fluid when performing an MIT. However, in some instances, a liquid testing fluid is used (Liquid-Liquid Interface test, LLI or LLMIT), when, for example, the wellhead was not designed to withstand the high gas pressures involved during a nitrogen MIT.

2. LLI and PD

Interpretation of a Liquid-Liquid Interface (LLI) tightness test using the Pressure Differential (PD) method can be described as follows. Well completion during a test includes a string and a cemented casing (Figure 2, left). Before the test, brine is injected in the well to increase its pressure. A light hydrocarbon (e.g., diesel oil) then is injected in the annular space to develop a brine/hydrocarbon interface in the cavern neck below the casing shoe of the last cemented casing. The PD method consists of monitoring the difference between the brine pressure and the hydrocarbon pressure, as measured at the wellhead. As a first approximation, hydrocarbon pressure and brine pressure distributions can be written

$$P_b(z,t) = P_b(0,t) + \gamma_b z \qquad \text{and} \qquad P_o(z,t) = P_o(0,t) + \gamma_o z$$

where $P_b(0,t)$ and $P_o(0,t)$ are brine pressure and hydrocarbon pressure measured at the wellhead $(z = 0)$, and γ_b and γ_o are brine and hydrocarbon pressure gradients, expressed in MPa/m.

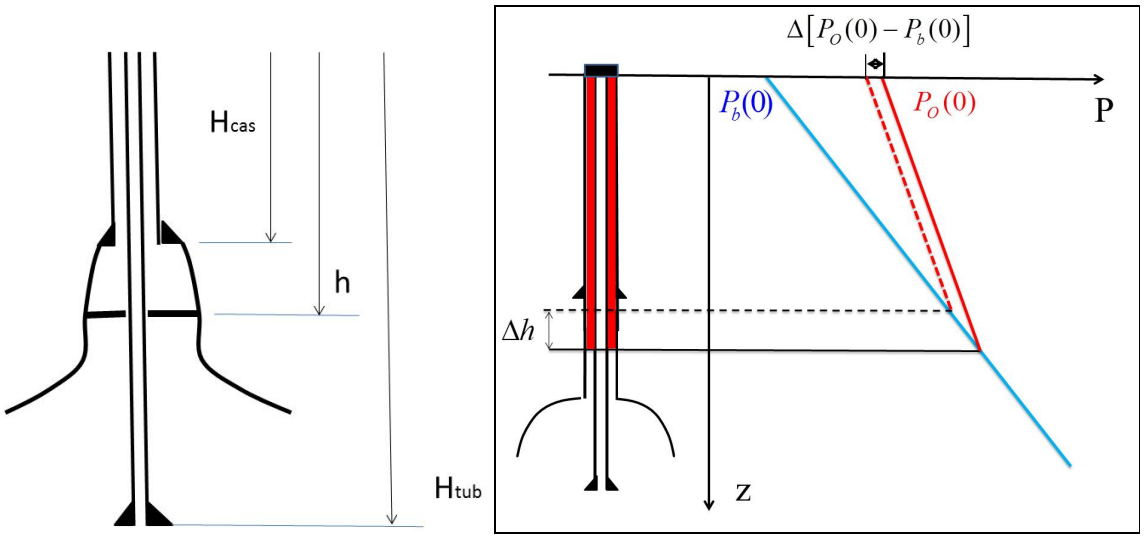

Figure 2. MIT and PD method.

At interface depth $(z=h)$, brine pressure and hydrocarbon pressure must be equal, $\left[P_b(h,t)=P_o(h,t)\right]$, and a change in the differential pressure is proportional to the rise of the interface (see Figure 2, right):

$$\dot{P}_o(t)-\dot{P}_b(t)=(\gamma_b-\gamma_o)\dot{h} \tag{1}$$

where, typically, $\gamma_b=0.012$ MPa/m and $\gamma_o=0.0083$ MPa/m.

Also, the hydrocarbon leak rate is proportional to the interface rise rate:

$$\dot{v}_{leak}=-\left[\frac{\dot{P}_o(t)-\dot{P}_b(t)}{\gamma_b-\gamma_o}\right]\Sigma(h) \tag{2}$$

where $\Sigma(h)$ is the cross-sectional area of the annular space at interface depth.

This method is simple: no interface depth measurement is needed. It is robust in that it is based on first principles (equilibrium equation in a fluid). Differential pressure evolution (and interface displacement evolution) are independent from cavern pressure evolution (at least in principle, see below) and can be recorded continuously (e.g., every second), providing additional insight in the behavior of the cavern and the borehole during the test.

Accurate pressure measurement is needed. A change in interface depth by $\Delta h=10$ cm (4 in) generates a relatively small differential pressure change, $\Delta P_o-\Delta P_b=2.7$ kPa. However, pressure sensors with resolutions of a few pascals are readily available, and a resolution of 1 cm is relatively easy to reach. When such a resolution is achieved, a more precise mathematical description of the

test is needed. When using Equations (1) and (2), it was assumed that pressure gradients γ_b and γ_o (i.e., oil and brine densities) are constant during the test. In fact, these fluids dilate or contract when cavern pressure or borehole temperature change. These effects are discussed in the next section.

3. Effects of Pressure and Temperature Changes

3.1. Pressure distributions in the borehole

The state equations of the fluids can be written

$$\gamma_o = \gamma_o^0\left[1+\beta_o\left(P-P_0\right)-\alpha_o\left(T-T_0\right)\right] \quad \text{and} \quad \gamma_b = \gamma_b^0\left[1+\beta_b\left(P-P_0\right)-\alpha_b\left(T-T_0\right)\right] \tag{3}$$

where, typically, $\beta_b = 2.7\times10^{-4}$/MPa, $\beta_o = 7\times10^{-4}$/MPa, $\alpha_b = 4.4\times10^{-4}$/°C, and $\alpha_o = 8\times10^{-4}$/°C. For each of the two fluids, the derivative with respect to time of the equilibrium equation,

$$\frac{\partial \dot{P}}{\partial z} = \gamma^0\left(\beta\dot{P}-\alpha\dot{T}\right) \tag{4}$$

can be integrated between the wellhead, where pressure rates are $\dot{P}_o\left(0,t\right)$ and $\dot{P}_b\left(0,t\right)$ respectively, and the interface depth, where pressure rates (when the interface depth is fixed) must equal the cavern-pressure rate, $\dot{P}_c(h,t)$:

$$\dot{P}_o\left(0,t\right) = e^{-\gamma_o\beta_o h}\left[\dot{P}_c\left(h,t\right)+\left(\gamma_b-\gamma_o\right)\dot{h}\right]+\int_0^h \gamma_o\alpha_o e^{-\gamma_o\beta_o z}\dot{T}_o\left(z,t\right)dz \tag{5}$$

$$\dot{P}_b\left(0,t\right) = e^{-\gamma_b\beta_b h}\dot{P}_c\left(h,t\right)+\int_0^h \gamma_b\alpha_b e^{-\gamma_b\beta_b z}\dot{T}_o\left(z,t\right)dz \tag{6}$$

At this step, simplifications can be made. Interface depth typically is $h = 1000$ m; $\gamma_o\beta_o h$ and $\gamma_b\beta_b h$ are smaller than 1%, and the differential pressure can be written as

$$\dot{P}_o\left(0,t\right)-\dot{P}_b\left(0,t\right) = \left(\gamma_b-\gamma_o\right)\dot{h}+\left(\gamma_b\beta_b-\gamma_o\beta_o\right)h\dot{P}_c(h,t)+\int_0^h\left[\gamma_o\alpha_o\dot{T}_o(z)-\gamma_b\alpha_b\dot{T}_b(z)\right]dz \tag{7}$$

The second and third terms in the right-hand side of Equation (7) account for the change in the weight of the two fluid columns due to cavern pressure and wellbore temperatures changes, which were disregarded in Equation (1).

3.2. Oil mass

The weight of the oil contained in the annular space is given by

$$mg = \int_0^h \Sigma(z)\ \gamma_o\left[P(z),T(z)\right]dz \tag{8}$$

and the leak rate is

$$-\dot{v}_{leak} = \frac{\dot{m}g}{\gamma_o^0} = \Sigma(h)\dot{h} + \int_0^h \left\{\left[\beta_0 \dot{P}_o(z) - \alpha_o \dot{T}_o(z)\right]\Sigma(z) + \dot{\Sigma}(z)\right\}\ dz \tag{9}$$

where $\Sigma(z)$ is the cross-sectional area of the annular space at depth z. In the following, its compressibility is neglected (when compared with oil compressibility), $\dot{\Sigma} = 0$; here, again, $\beta_o \gamma_o h$ is assumed to be much smaller than 1. When no leak is assumed,

$$0 = \Sigma(h)\dot{h} + v_0\beta_0\dot{P}_c(t) - \int_0^h \alpha_o \dot{T}_o(z)\Sigma(z)dz \tag{10}$$

where v_o is the volume of the oil in the annular space. In Equation (10), the second and third terms reflect the effects on oil volume of the changes in cavern pressure and oil temperature.

3.3 Oil and brine volume changes

Cavern pressure changes, $\dot{P}_c(h,t)$, and temperature changes, $\dot{T}_o(z,t)$ and $\dot{T}_b(z,t)$, generate changes in oil and brine volumes, as reflected by Equation (10). However, these changes are exceedingly small when compared to cavern brine volume, and they are not able to exert a significant influence on cavern pressure, whose changes are due mostly to external factors such as thermal expansion of cavern brine, cavern creep closure, etc. For this reason, $\dot{P}_c(h,t)$, $\dot{T}_o(z,t)$ and $\dot{T}_b(z,t)$ are considered independent variables.

4. Apparent Leaks Generated by Cavern Pressure Change

In this section, the effects of cavern pressure change during the test are discussed; oil and brine temperatures are assumed to remain constant during the test.

4.1. Interface displacement generated by cavern pressure change

Consider the case in which a logging tool is used to measure interface depth (standard LLI test). A change in cavern pressure (ΔP_c) generates a change in interface depth, Δh; hence, there is an apparent leak, $\Delta v_{leak}^{app;tool}$, such that

$$\Delta v_{leak}^{app;tool} = -\Sigma(h)\Delta h = v_0 \beta_0 \Delta P \tag{11}$$

For instance, the volume of a 1000-m long, 9″5/8×13″3/8 annular space is $v_o = 40\ \mathrm{m}^3$ (no neck assumed), and

$$\Delta v_{leak}^{app;tool}\ [\mathrm{liters}] = -\Sigma(h)\Delta h = -28\Delta P_c\ [\mathrm{MPa}].$$

The error is still larger when the testing fluid is propane, which is more compressible than diesel oil.

4.2. Additional apparent leak generated by the PD calculation method

Consider the case that a leak is assessed through the PD method:

$$\Delta v_{leak}^{app;PD} = -\frac{\Delta P_0(0,t) - \Delta P_b(0,t)}{\gamma_b - \gamma_o}\Sigma(h) = \Delta v_{leak}^{app;tool} - \left(\frac{\gamma_b \beta_b - \gamma_o \beta_o}{\gamma_b - \gamma_o}\right) h\Sigma(h)\Delta P_c \tag{12}$$

and an additional apparent leak is generated (associated with no interface displacement) when using the PD method to compute the leak:

$$\Delta v_{leak}^{app;PD}\left[\mathrm{liters}\right] = \Delta v_{leak}^{app;tool} + 0.695\ \Sigma(h)\Delta P_c\left[\mathrm{MPa}\right]$$

4.3. Example

Figure 3 displays the results the results of an MIT test performed in an AkzoNobel cavern. Interface depth was 453 m. In addition to a logging tool, the Pressure Differential method was used: diesel-oil and brine pressure were recorded at ground level. At hour 3.2, brine was injected in the cavern to restore the initial testing pressure. Cavern pressure increased by $\Delta P_c = 0.2\ \mathrm{MPa}$. The green curve displays the interface depth evolution, as computed through Equation 1 (no correction). The red curve displays the "actual" interface displacement, taking into account the additional term described in Section 3.4.2 (Equation 11). The blue curve accounts for the correction described in Section 3.4.1 (Equation 12). It is this blue curve that must be considered when discussing a level rise corrected for pressure decrease (In this case, it is possible that the slow rise of the blue curve is due to thermal effects, as discussed in the next Sections).

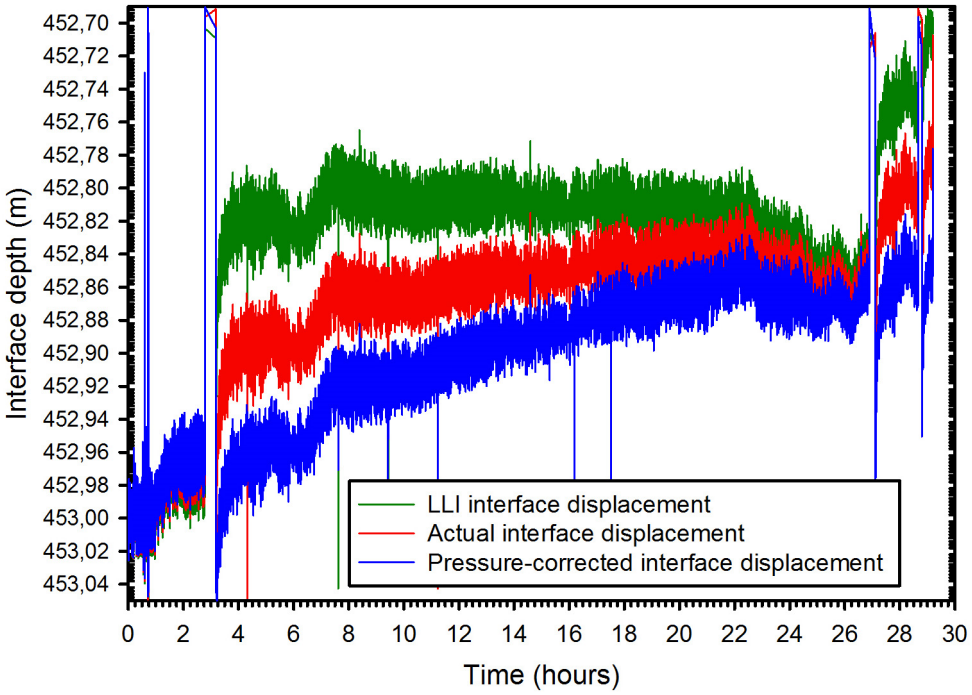

Figure 3. Interface displacement during an MIT. (Acknowledgements: AkzoNobel)

5. The Apparent Leak Generated by Wellbore Temperature Changes

5.1. Origin of temperature changes.

In this Section, cavern pressure is assumed to remain constant during the MIT. Equations (7) and (9) can be rewritten

$$0 = \Sigma(h)\Delta h - \int_0^h \alpha_o \Delta T_o(z,t)\Sigma(z)dz \tag{13}$$

$$\Delta P_o(0,t) - \Delta P_b(0,t) = (\gamma_b - \gamma_o)\Delta h + \int_0^h \left[\gamma_o \alpha_o \Delta T_o(z,t) - \gamma_b \alpha_b \Delta T_b(z,t)\right] dz \tag{14}$$

As in the case of the effects of cavern pressure discussed above, Equation (13) describes the (actual) interface depth change due to oil warming or cooling, which leads to an apparent leak by

$$\Delta v_{leak}^{app;tool} = -\Sigma(h)\Delta h \tag{15}$$

Equation (14) describes the additional apparent leak that appears when the PD method is used to compute the leak:

$$\Delta v_{leak}^{app;PD} = -\frac{\Delta P_o(0,t) - \Delta P_b(0,t)}{\gamma_b - \gamma_0}\Sigma(h) = \Delta v_{leak}^{app;tool} - \frac{\Sigma(h)}{\gamma_b - \gamma_o}\int_0^h \left[\gamma_o \alpha_o \Delta T_o(z,t) - \gamma_b \alpha_b \Delta T_b(z,t)\right] dz \tag{16}$$

In a wellbore that had been kept idle over a long period of time, oil and brine temperatures are in equilibrium with the geothermal temperature of the rock mass. However, the following are noted.

- When the cavern is leached out, cold water is injected in the cavern through the central string. In the cavern, brine is formed and slowly warms for two main reasons: heat is transferred from the rock mass to the cavern and salt dissolution is an exothermic process. The warm brine then flows upward as heat is transferred from the rock mass to the cavern. In addition, salt dissolution is an exothermic process: warm brine flows upward through the annular space and exchanges heat with cold water flowing downward. For this reason, at ground level, brine temperature is not very different from water temperature. However, at depth, wellbore temperature is significantly colder than rock mass temperature. After solution mining is completed, the temperature gap slowly decreases; it vanishes after a time period comparable to the solution mining duration.

- Day/night and summer/winter temperature changes at ground level are transmitted to the upper part of the well. The values of the integrals

$$\int_0^h \Delta T_o(z,t)dz \quad \text{and} \quad \int_0^h \Delta T_b(z,t)dz$$

  are several dozens of °C×m (respectively, several hundreds of °C×m) when daily (respectively, yearly) temperature changes are considered. In addition, a time lag can be observed: the two integrals do not reach their maximum values at the same time. For this reason, fluctuations of the differential pressure can be observed at ground level (Van Sambeek et al., 2005; Olesko et al., 2012, p. 11, Figure 7).

- During an MIT, cold brine (and cold testing fluid) are injected in the cavern during the pre-pressurization phase. This is discussed in more details in the following.

Note that the effects of these temperature changes can be significant. Assume, for instance, that the oil temperature is colder than the geothermal temperature by $\Delta T_o = 10°\text{C}.$ Oil warms slowly to reach equilibrium with the rock mass. The annular cross-section is $\Sigma(z) = 40 \text{ liters/m},$ and the interface depth is $h = 1000 \text{ m}.$ According to Equation (13), oil warming will lead to an apparent negative leak of – 320 liters. (The interface drops down into the neck).

5.2. Effects of temperature changes during an MIT

During a typical MIT, four phases can be distinguished:

(1) Phase 1: Brine injected in the central string to pre-pressurize the cavern;

(2) Phase 2: Stabilization period;

(3) Phase 3: Testing fluid injected in the annular space; and

(4) Phase 4: Integrity test.

The thermal description of these four phases is provided in more detail in the Appendix.

During Phases 1 and 3, oil and brine temperatures are assumed to be radially uniform: $T_b = T_b(z,t)$ and $T_o = T_o(z,t)$. Heat transfer (which is assumed to be purely horizontal) results from conduction through the rock mass, conduction through the steel casing and the steel string, and through convection.

During Phases 2 and 4, there is no fluid movement in the wellbore, convection (a major contributor to heat transfer) vanishes, and a more precise description of heat transfer through the fluids is needed. Heat transfer results from conduction through the rock mass, through the steel casing and through the fluids, $T_b = T_b(z,r,t)$ and $T_o = T_o(z,r,t)$. A similar approach was adopted by Lampe and Ratigan (2014).

The following assumptions were made. Wellbore length is $h = 1000\ \mathrm{m}$, cavern volume is $V = 500{,}000\ \mathrm{m}^3$, and cavern compressibility is $\beta V = 200\ \mathrm{m}^3/\mathrm{MPa}$. During pre-pressurization, a 1200-m^3 volume of brine is injected in the cavern to increase its pressure by 6 MPa. Phases 1, 2, 3 and 4 last 24 h, 4 h, 24 h and 5 days, respectively. The brine flow-rate during pre-pressurization is $Q_b = 50\ \mathrm{m}^3/\mathrm{h}$, and the brine velocity is $u' = 0.66\ \mathrm{m/s}$. The diesel-oil celerity during Phase 3 is 0.66 m/s. Well completion includes a 7″ string and a 9$^{5/8}$″ casing, with respective thicknesses of 0.72 cm and 2.14 cm. For simplicity, the cross-sectional area at interface depth (''cavern neck'') is the same as at any depth in the wellbore, $\Sigma(h) = \Sigma(z)$. The thermal conductivities of steel, rock, diesel oil and brine are 30 W/m-°C, 5 W/m-°C, 0.3 W/m-°C, 1.06 W/m/°C, respectively (the two last figures being slightly too high). The heat capacities of brine and diesel oil are 3500 J/kg-°C and 1670 J/kg-°C, respectively. The rock mass includes a 500-m-thick overburden layer and a 500-m-thick salt layer. The geothermal temperature is 12 °C at ground level, 34 °C at a 500-m depth and 45 °C at a 1000-m depth. The thermal expansion coefficients of the oil and brine are $\alpha_0 = 8.2\times10^{-4}/°\mathrm{C}$ and $\alpha_b = 4.4\times10^{-4}/°\mathrm{C}$, respectively.

5.3. First example: Injected fluid temperature equals ground-level temperature

Consider the case in which the temperatures of the brine and oil injected in the wellbore equal the ground-level temperature (12°C). Figure 4 displays brine temperature in the string during Phases 1, 2, 3 and 4, respectively. During Phase 1, brine temperature decreases (except at ground level) as cold brine is injected in the well; steady-state temperature is not reached even after 24 hours. The distribution reached after 24 hours is the initial distribution of Phase 2: during the 24-h-long

stabilization period, brine slowly warms. However, even after 24 hours, brine temperature is significantly colder than the geothermal temperature. During diesel-oil injection (Phase 3), brine cools again, but this effect is small, as oil injection is short (30 minutes) and the oil-heat capacity is smaller than that for brine. During the MIT, brine (and oil) temperatures slowly increase, generating an apparent negative leak (Figure 5).

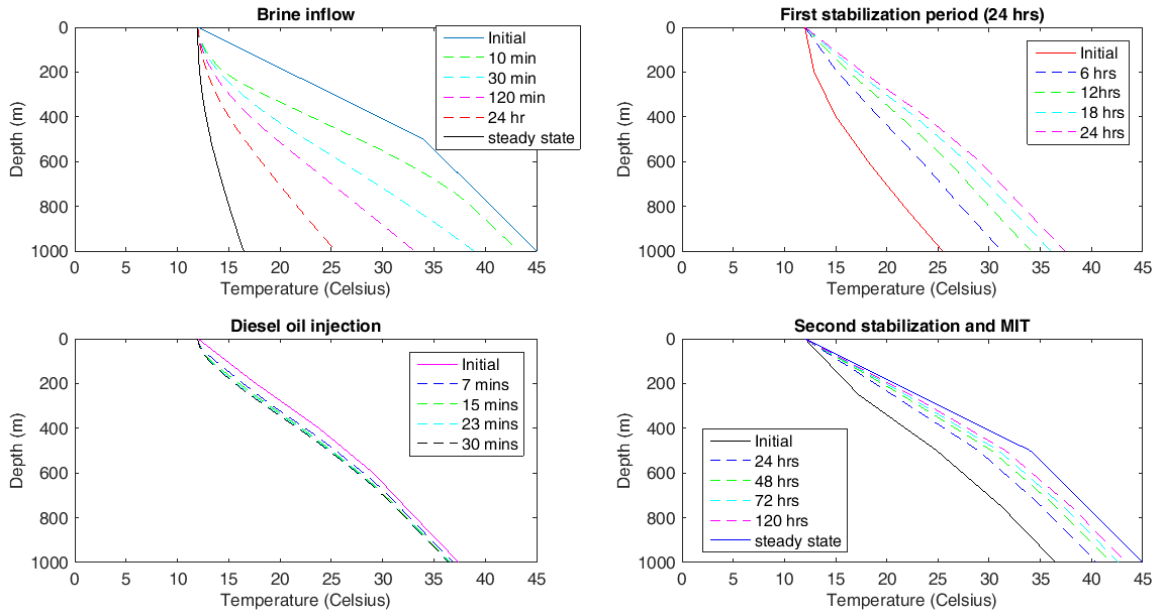

Figure 4. Temperature evolution during Phases 1 (top left), 2 (top right), 3 (lower left) and 4 (lower right) (The temperature of the injected fluids is 12 °C.)

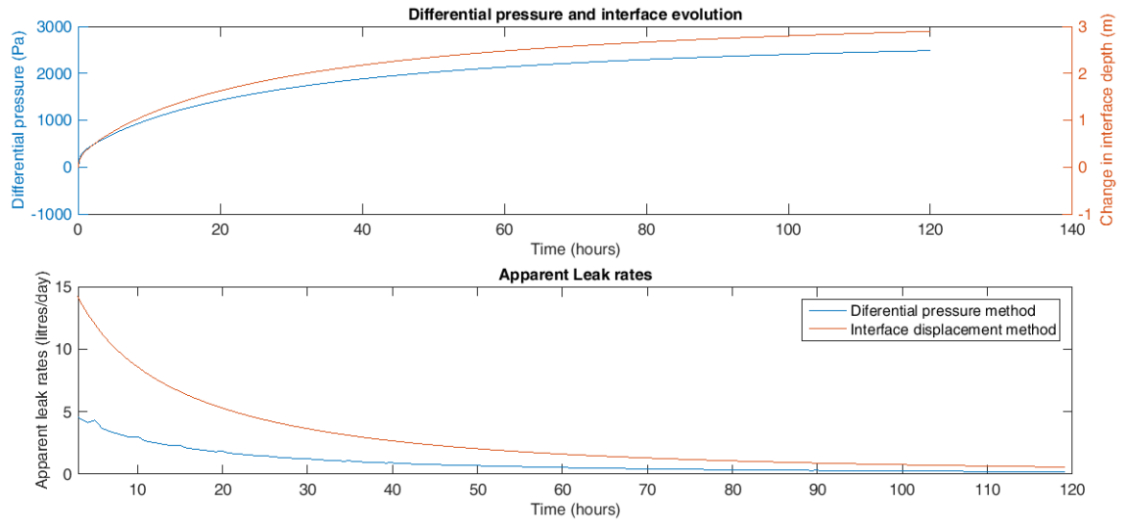

Figure 5. Differential pressure evolution, interface evolution and apparent leak rates during the MIT (injection temperature = 12°C).

5.2. Second example: Injected fluids temperature is warmer than ground level temperature

Consider the case when the temperatures of the brine and oil injected in the wellbore is 32 °C. Figure 6 displays brine temperature in the string during Phases 1, 2, 3 and 4, respectively. At the beginning of Phase 1, the injected warm brine pushes a cold column of brine to the bottom of the well. At the end of this phase, brine temperature is warmer than geothermal temperature in the upper part of the wellbore; the inverse is true in the lower part of the wellbore. During the stabilization period, the virgin temperature is restored slowly. During oil injection, brine temperature increases in the upper part of the wellbore and decreases in the lower part as relatively cold brine is pushed to the bottom of the wellbore. During Phase 4, the virgin distribution of temperature slowly is restored, but the brine remains significantly warmer in the upper part of the well. The history of the apparent-leak rates is more complex than in the first example (when the injection temperature equals 12 °C): after one day, the apparent leak rates generated by thermal effects are negative (Figure 7).

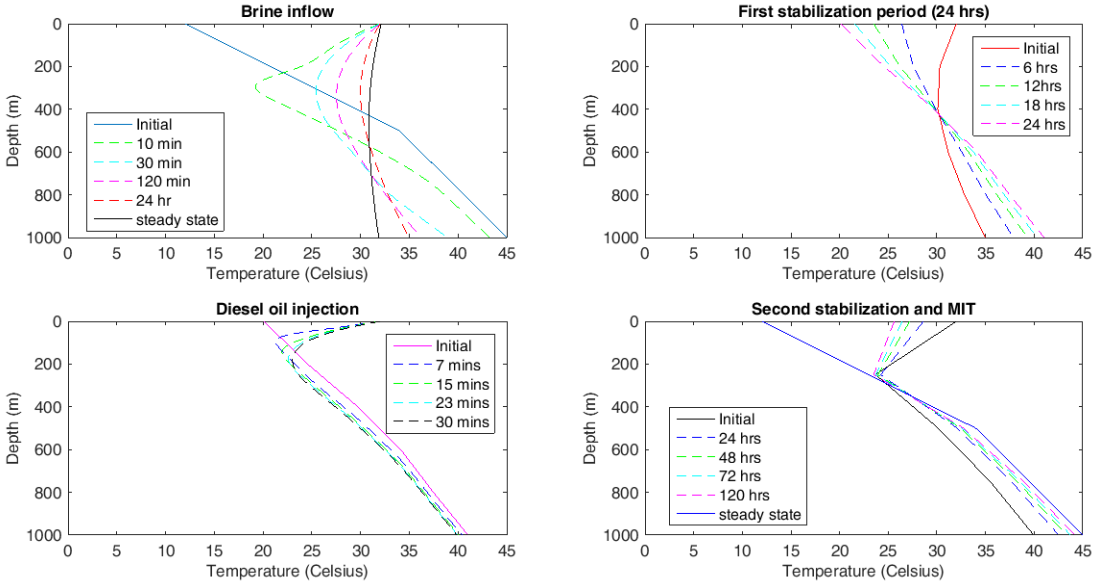

Figure 6. Temperature evolution during Phases 1 (top left), 2 (top right), 3 (bottom left) and 4 (bottom right). (The temperature of the injected fluids is 32 °C.)

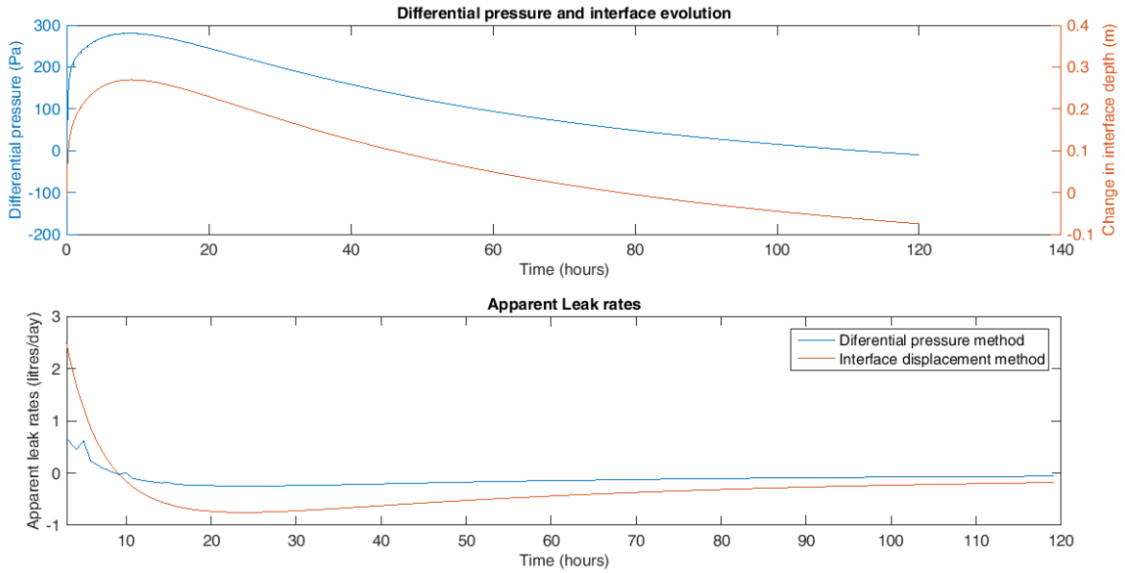

Figure 7. Differential pressure evolution, interface evolution and apparent leak rates during the MIT (injection temperature = 32 °C).

References

Bérest P., Brouard B., Durup J.G. (2001). *Tightness Tests in Salt-Cavern Wells*. Oil & Gas Science and Technology – Rev. IFP, Vol.56 (2001), n°5, 451-469.

Crotogino F.R. (1996). *SMRI references for external well mechanical integrity testing/performance, data evaluation and assessment*, Summary of the final project report, SMRI 94-0001. SMRI Spring Meeting, Houston, Texas.

Diamond H.W., Bertram B.M., French P.S., Petrick G.D., Schumacher M.J., Smith J.B. (1993). *Detecting very small casing leaks using the water-brine interface method*. Proc. 7th Symp. on Salt, Vol. I. Amsterdam: Elsevier Science Publishers B.V., 363-368.

Lampe B., Ratigan J.L. (2014). *Pitfalls of a Nitrogen-Brine interface Mechanical Integrity Test*. SMRI Spring Meeting, San Antonio, 19-30.

Langlinais J., Moran T. (2008). *Using a downhole camera to monitor the Nitrogen Interface during an MIT – Experience at Gaines County, Texas*. SMRI Fall Meeting, Galveston, Texas, 167-173.

Meinecke I., Walter M., Kruck O. (2013). *A Hydraulic Mechanical Integrity Test of an oil cavern using the SoMIT method*. SMRI Fall Meeting, Avignon, France, 221-230.

Olesko M., Ratigan J., Skaug N. (2012). *Application of the Liquid-Liquid Interface Mechanical Integrity Test to Bedded Salt Solution-Mined Hydrocarbon Storage Cavern Wells*. SMRI Spring Meeting, Regina, Saskatchewan, Canada, 139-153.

Skaug N.T., Ratigan J.L., Lampe B.C. (2011). *A critical look at the Nitrogen/Brine Interface Mechanical Integrity Test*. SMRI Fall Meeting, York, UK, 324-332.

Van Sambeek L.L., Bérest P., Brouard B. (2005). *Improvements in Mechanical Integrity Testing for Solution Mined Caverns used for Mineral Production or liquid-product storage*. *Topical Report RSI-1799*, prepared for the Solution Mining Research Institute.

Vrakas J. (1988). *Cavern integrity testing on the SPR program*. SMRI Spring Meeting, Mobile, Alabama.

Acknowledgments

This work is a part of an ongoing study supported by the French Agence Nationale de la Recherche *(ANR)* in the framework of the FluidStory Project, devoted to storage of oxygen and CO_2 in salt caverns. AkzoNobel kindly authorized the reproduction of pressure measurement records. The authors benefited from helpful discussions with Tjeerd Koopmans and Tobias Pinkse, from AkzoNobel, and Arnaud Réveillère from Geostock. Special Thanks to K. Sikora.

APPENDIX

During an MIT, four phases can be distinguished:

(1) Brine injected in the central string to pre-pressurize the cavern;

(2) Stabilization period;

(3) Test fluid injected in the annular space; and

(4) Integrity test.

The mathematical description of these four phases is provided in the following.

At the beginning of phase 1, temperature is uniform at any depth:

$$T_R(r,z,t) = T_b(r,z,t) = T_o(r,z,t) = T_\infty(z,r_\infty) = T_0 + Gz$$

It is assumed that heat fluxes are horizontal. For this reason, variable z will be omitted. The tubing, whose internal and external radii are *a* and *b*, respectively, and the casing, whose internal and external radii are *c* and *d*, respectively, are thin (1 cm); they are composed of steel whose thermal conductivity is large ($K_{steel} = 45$ W/m-°C is typical): steady state is reached rapidly and the heat fluxes in the tubing and casing are uniform:

$$q_{R\to ann} = K_{steel}\frac{T_R(d,t) - T_o(c,t)}{e_{cas}} \quad \text{and} \quad q_{ann\to tub} = -q_{tub\to ann} = K_{steel}\frac{T_o(b,t) - T_b(a,t)}{e_{tub}} \qquad \text{(A1)}$$

Conduction takes place in the rock mass:

$$\frac{\partial T_R(r,t)}{\partial t} = k_R\left[\frac{\partial^2 T_R}{\partial r^2} + \frac{1}{r}\frac{\partial T_R}{\partial r}\right] \qquad T_R(r_\infty,t) = T_\infty(z) \qquad -K_R\frac{\partial T_R(d,t)}{\partial r} = q_{R\to ann}(t) \qquad \text{(A2)}$$

When the temperature of the testing fluid (diesel oil, for example) at the casing inner wall ($r = c$) is kept constant and equal to 1 after $t = 0$, $T_o(c, t > 0) = 1$, the heat flux in the steel casing can be computed, $q_{R\to ann} = \varphi(t)$, and, for any oil-temperature evolution at the casing inner wall, the heat flux can be computed through a convolution:

$$q_{R\to ann} = \int_0^t T_o(c,\tau)\ \varphi(t-\tau)\ d\tau \qquad \text{(A3)}$$

Phase 1. Brine flow, no oil flow

During this phase, the oil remains standstill in the annular space; however, brine flows downward in the central tubing of length H, with a velocity of $u = Q_b / S_{tub}$, where Q_b is the brine-flow rate, and S_{tub} is the cross-sectional area of the central tubing. During this phase, it is assumed that testing fluid temperature and brine temperature are radially uniform.

Two heat balance equations can be written:

$$\rho_b C_b \pi a^2 \frac{dT_b}{dt} = 2\pi a q_{ann\to tub} \tag{A4}$$

$$\rho_o C_o \pi \left(c^2 - b^2\right) \frac{\partial T_o}{\partial t} = 2\pi b q_{tub\to ann} + 2\pi c q_{R\to ann} \tag{A5}$$

The second equation can be interpreted as follows. The temperature of the diesel oil changes, as diesel oil receives a heat flux from both the central tubing and the steel casing. Note that a *partial* derivative with respect to time is used because oil remains standstill in the annular space.

The first equation stipulates that brine temperature changes as it receives heat from the annular space through the steel tubing. However, the derivative with respect to time is *total* — i.e., this relation is true only when one considers a particle of brine flowing along the tubing with the velocity *u*. In other terms, this relation is only true along a *characteristic* line, $z - ut = c$ and $dT_b/dt = \partial T_b/\partial t + u\,\partial T_b/\partial z$.

To solve the differential equations, boundary conditions are needed. Along a *c*-line such that $c > 0$ (which describes the movement of a brine particle that was in the well before the test), this condition is $T_b(z = C, 0) = T_\infty + Gc$. Along a *c*-line such that $c < 0$ (which describes the movement of a brine particle which was injected in the well), this condition is $T_b(z = 0, t = -C/u) = T_b^{inj}$, where T_b^{inj} is the temperature of the injected brine.

A possible numerical procedure is as follows. A space-step is selected, $\Delta z = H/N$, and the time step is $\Delta t = \Delta z/u$. It is assumed that $T_o(z = j\Delta z, t = n\Delta t)$ and $T_b(z = j\Delta z, t = i\Delta t)$ are known for any $0 \le j \le N$ and any $0 \le i \le n$. This allows computing the convolution (A3) — i.e., the value of $q_{R\to ann}(j\Delta z, n\Delta t)$, hence the values of $T_o(z = j\Delta z, t = (n+1)\Delta t)$ and $T_b(z = j\Delta z, t = (n+1)\Delta t)$.

Phase 2. No flow

At the beginning of Phase 2, brine injection stops. Now brine and oil temperatures are radially uniform, and rock temperature is a function of the distance to the well axis. Brine and oil remains standstill. In such conditions, thermal conduction in the fluids no longer can be neglected:

$$\frac{\partial T_o(r,t)}{\partial t} = k_o \left[\frac{\partial^2 T_o}{\partial r^2} + \frac{1}{r}\frac{\partial T_o}{\partial r} \right] \qquad \text{and} \qquad \frac{\partial T_b(r,t)}{\partial t} = k_b \left[\frac{\partial^2 T_b}{\partial r^2} + \frac{1}{r}\frac{\partial T_b}{\partial r} \right]$$

Boundary conditions can be written:

$$-K_b \frac{\partial T_b}{\partial r}(a,t) = q_{ann\to tub}(t)$$
$$+K_o \frac{\partial T_o}{\partial r}(b,t) = q_{tub\to ann}(t)$$
$$-K_o \frac{\partial T_o}{\partial r}(c,t) = q_{R\to ann}(t)$$

When the flow of heat to the tubing is kept constant and equal to 1 after $t=0,\ q_{ann\to tub}=1,\ t>0,$ and the brine temperature is $\psi(r,t).$ When $q_{tub\to ann}=1,\ t>0,\ \ q_{R\to ann}=0,\ t>0,$ and the oil temperature is $\chi_R(r,t).$ When $q_{R\to ann}=1,\ t>0,\ \ q_{ann\to tub}=0,\ t>0,$ oil temperature is $\chi_{tub}(r,t).$ For any heat flux, oil and brine temperatures can be computed through a convolution:

$$T_o(r,t) = \int_0^t q_{R\to ann}\chi_R(t-\tau) + q_{tub\to ann}(\tau)\chi_{tub}(t-\tau)d\tau.$$

$$T_b(r,t) = \int_0^t q_{ann\to tub}(\tau)\psi(t-\tau)d\tau$$

Phase 3. Oil flow, no brine flow

The equations now are

$$\rho_b C_b \pi a^2 \frac{\partial T_b}{\partial t} = 2\pi a q_{ann\to tub}$$
$$\rho_o C_o \pi (c^2 - b^2)\frac{dT_o}{dt} = 2\pi b q_{tub\to ann} + 2\pi c q_{R\to ann}$$

The same method as for Phase 1 can be used. However, oil velocity is $u' = Q_o / S_{ann}$, where Q_o is the oil-flow rate, and S_{ann} is the annular cross-sectional area.

Phase 4. No flow

The same method as for Phase 2 can be used.

The functions $\chi_{tub}(r,t),\ \chi_R(r,t),\ \psi(r,t),\ \varphi(t),$ which are needed to compute the solutions, can be determined through the separation of variables method. These functions can be expressed as a series of Bessel functions. For the computations presented in this paper, the first hundred terms were used.